Journal of CO2 Utilization 110 (2026) 103478

Contents lists available at ScienceDirect

Journal of CO2 Utilization

journal homepage: www.elsevier.com/locate/jcou

Techno-economic assessment framework for industrial CO_2 utilization in e-methanol synthesis: Integrating capture, liquefaction, storage and multi-modal transport

Javier Vendrell-Granero [a], Ahmed M. Elberry [b], Sayan Das [c], Jagruti Thakur [a,*]

[a] Department of Energy Technology, KTH Royal Institute of Technology, Stockholm, Sweden
[b] Faculty of Science (HIMS), University of Amsterdam, Amsterdam, the Netherlands
[c] Karlsruhe Institute of Technology, Germany

ARTICLE INFO

Keywords:
E-methanol
CO_2 supply chain
Carbon capture
Utilization and storage
LCOeM
Techno-economic assessment
CO_2 transport
Biogenic CO_2

ABSTRACT

Achieving deep decarbonization in hard-to-abate sectors requires scalable low-carbon fuels derived from biogenic or air-captured CO_2. E-Methanol is a promising option, but its deployment depends on robust CO_2 value chains that integrate industrial emissions, conditioning, multi-modal transport and reliable supply of power. Despite progress in carbon capture research, integrated assessments combining real emitters, CO_2 logistics, storage design, downtime-driven oversizing and transport fleet operations remain unavailable, limiting accurate levelized cost prediction of e-fuel value chain. The study proposed a unified framework to evaluate the techno-economic feasibility of the overall CO_2-to-e-methanol chain, integrating capture, liquefaction, storage, different transport possibilities and final synthesis. Results show that CO_2 availability strongly determines feasible plant size, while transport mode significantly shapes logistics cost. E-methanol synthesis is the largest contributor, with the Portuguese cement scenario yielding 1111.3 €/t. Across the analysed scenarios, maritime transport usually delivers 51–60% lower cost than road transport. The framework supports rigorous planning of CCU-enabled e-fuel synthesis.

1. Introduction

Methanol plays a central role in the transition toward low-carbon energy systems as both a chemical feedstock and an energy carrier. Conventionally, methanol is produced from fossil-based routes such as natural gas reforming and coal gasification, which are associated with significant carbon dioxide (CO_2) emissions. In recent years, alternative pathways including biomass gasification, waste-to-methanol conversion, and CO_2 hydrogenation have been extensively studied from both technical and economic perspectives. For instance, techno-economic analyses of plasma-assisted waste gasification integrated with CO_2 utilization demonstrate production costs in the range of 500–620 €/t, highlighting the growing competitiveness of circular carbon pathways [1]. Despite these advances, the economic performance of different methanol synthesis routes remains highly sensitive to feedstock type, hydrogen and electricity costs, and system integration.

The urgent need to mitigate climate change has accelerated the global transition from fossil-based energy systems toward sustainable and renewable alternatives [2]. The industrial sector is a major contributor to global CO_2 emissions, making it a key target for decarbonizing efforts [3]. However, reducing emissions from industry is particularly challenging, as many industrial processes intrinsically generate CO_2 or depend on carbon-based feedstocks, limiting the effectiveness of electrification-based solutions. These hard-to-abate sectors, including cement, steel, and chemicals, require integrated mitigation strategies beyond direct energy substitution [4].

In this context, Carbon Capture, Utilization, and Storage (CCUS) has emerged as a key enabler for achieving deep decarbonization [4,5]. CCUS systems enable the capture of CO_2 from industrial processes and its subsequent utilization or permanent storage, thereby reducing net emissions [6]. Recent studies highlight that CCUS deployment is strongly influenced by spatial heterogeneity, infrastructure availability and policy incentives [7]. For example, investment decisions for CCUS retrofits in coal-fired power plants depend on source–sink matching and economic uncertainties, emphasizing the importance of integrating transport and storage considerations into system design. Similarly,

* Corresponding author.
E-mail address: jrthakur@kth.se (J. Thakur).

https://doi.org/10.1016/j.jcou.2026.103478
Received 24 March 2026; Received in revised form 15 May 2026; Accepted 30 May 2026
Available online 20 June 2026

plant-level analyses in the cement industry demonstrate that regional differences and policy incentives significantly affect CCUS feasibility and deployment strategies. In addition, the availability of geological CO_2 storage capacity and injection rates plays a crucial role in determining long-term system viability. Complementary integration of renewable energy systems, such as wind–solar–hydro combinations, further supports CCUS and Power-to-X pathways by enabling a stable and low-carbon energy supply for hydrogen production. These findings highlight the need for region-specific, integrated techno-economic frameworks that capture the interactions between CO_2 sources, transport infrastructure, storage capacity, and energy systems [8].

While Carbon Capture and Storage (CCS) focuses on long-term sequestration, Carbon Capture and Utilization (CCU) enables the conversion of CO_2 into value-added products, supporting circular carbon economy concepts and improving economic viability [8]. Conventional approaches have largely focused on CCS technology; however, its implementation is often constrained by geographic availability and geological suitability and high associated cost [9]. In contrast, the CCU pathway treats CO_2 as a valuable carbon resource that can be reintegrated into the economic cycle. The CO_2 can be utilized through physical, chemical or biological conversion routes, enhancing market viability and supporting long-term deployment [10].

Within this broader context, e-methanol (e-MeOH) synthesized via hydrogenation of captured CO_2 has emerged as a promising pathway for sustainable fuel synthesis [11]. Methanol is widely used in the chemical industry and is increasingly considered as an alternative fuel for transportation sectors such as shipping and aviation [12]. However, current methanol synthesis remains predominantly fossil-based, with approximately 65% derived from natural gas and the remainder from coal, both of which contribute significantly to global emissions [13]. Transitioning toward renewable methanol pathways is therefore essential to reduce lifecycle emissions and support industrial decarbonization [14,15]. The synthesis of e-MeOH requires green hydrogen and eligible CO_2 sources, including biogenic, geogenic, and air-captured CO_2, in accordance with evolving regulatory frameworks [16].

1.1. Research gaps

Despite the growing interest in CCU pathways and e-MeOH synthesis, several critical gaps remain in the existing literature (see Table 1).

Table 1
State-of-the-art for techno-economic assessment of e-MeOH.

Authors and year	Proposed objectives	Limitations
Farfan et al., 2019 [9]	Proposes a global potential analysis of CCU as a possible solution for the CO_2 emissions of cement production	No modelling of CO_2 transport infrastructure, fleet size, or intermediate storage
Salkuyeh K et al., 2021 [12]	Detailed process modelling of e-MeOH	Assumes CO_2 availability; transport ignored
Yang et al., 2021 [17]	Industrial CCS cost comparison	no modelling of CO_2 logistics chains or utilization pathways.
Fraga et al., 2021 [18]	Detailed storage and hub design "A mixed-integer linear programming optimisation model has been developed for sizing and costing intermediate storage hubs of CO_2"	No utilisation; no fuel synthesis
Sollai et al., 2023 [19]	Levelized cost of e-methanol (LCOeM) driven by H_2 and power	CO_2 treated as generic input
Emanuelsson et al., 2025 [20]	EU-level CCS deployment analysis with aggregated transport assumptions;	no operational logistics modelling
Noh and kang, 2025 [21]	Detailed CO_2 ship transport economics; Onboard reliquefaction	Transport-only study

Most studies treat CO_2 as a generic or constant input, neglecting the spatial and temporal variability of industrial emissions. In addition, the studies often neglect critical system elements such as comparing multimodal transport networks, loop-time and fleet-size constraints, and downtime-driven buffer storage requirements. Additionally, the operation interdependencies among capture, condition, transport and utilization stages are omitted from the evaluation. Moreover, few works benchmark tanker-based and truck-based CO_2 transport within the same system boundary, and fewer quantify how these infrastructure choices jointly influence the levelized cost of CO_2 and e-MeOH. These gaps limit the reliability of techno-economic planning for large-scale e-MeOH deployment tailored to specific industrial clusters.

1.2. Research objectives

The primary objective of this study is to develop a realistic and comprehensive assessment of the CO_2-to-e-MeOH supply chain to support large-scale industrial and maritime transportation decarbonization, specifically by identifying the most competitive combinations of industrial CO_2 emitters and transport configurations for supplying a coastal power-to-liquid (PtL) e-MeOH facility. The study quantifies it by estimating the levelized cost of CO_2 and e-MeOH. By focusing on industrial point sources, the work addresses a critical need for identifying feasible CO_2 supply pathways capable of delivering both emissions reductions and a valuable renewable fuel. To achieve this proposed objective, the study performed an end-to-end techno-economic assessment that models the full CU chain using real industrial conditions. The methodology integrates spatially distributed emitters, capture systems, liquefaction units, intermediate storage sizing and compares maritime and road-based transport modes. Industrial-scale CO_2 flow constraints are combined with multi-stage process modelling, enabling the evaluation of feasible e-MeOH plant capacities. Furthermore, this framework includes downtime-driven oversizing requirements and transparent stage-wise cost allocation to assess how logistical and operational factors influence the overall economics of the e-MeOH synthesis. The novelty of this work lies in its realistic and system-level representation of the CO_2 supply chain, which goes beyond the simplified assumptions commonly used in earlier studies.

2. Materials and methodology

2.1. E-MeOH synthesis process

Synthetic fuels such as e-MeOH hold significant potential to displace conventional fossil fuels and thereby support a broader shift toward a low-carbon energy system. As a result, biogenic CO_2 is projected to become a valuable commodity, contributing to both circular carbon strategies and emerging fuel markets. This growing demand creates new opportunities for a wide range of biogenic CO_2 sources, including ethanol plants, biomass power facilities, waste-to-energy plants, cement manufacturing, pulp and paper mills, alcohol and sugar production facilities, and biogas plants, to supply CO_2 for sustainable fuel synthesis. The main reactions occurring are shown in Eqs. 1–3 [19]:

$$CO_2 + 3H_2 \leftrightarrow CH_3OH + H_2O \quad (1)$$

$$CO_2 + H_2 \leftrightarrow CO + H_2O \quad (2)$$

$$CO + 2H_2 \leftrightarrow CH_3OH \quad (3)$$

The process utilizes hydrogen to convert biogenic, geogenic or air captured CO_2 into methanol, thereby reducing emissions, promoting resource circularity and contributing to industrial decarbonization. By closing the carbon loop and enabling the valorisation of captured CO_2, e-MeOH synthesis offers a compelling solution for sustainable industrial transformation. Approximately 45% of the total methanol is consumed by the chemical industry, while 11% is considered as an alternative fuel

in the transportation sector [2]. Considering this growth of e-MeOH as an energy carrier, it is projected in the studies that the global e-MeOH production will surpass 120 million tonnes, due to its potential to support energy diversification and decarbonization [19]. Therefore, with the increasing demand for e-MeOH, the improvement of techno-economic efficiencies of this low-carbon fuel becomes critical. This study evaluates the full CCU supply chain required to provide CO_2 feedstock to an e-MeOH synthesis plant. Fig. 1 depicts the overall value chain of this study.

2.2. Schematic model description

The schematic arrangement is structured around the sequential stages of the CCU value chain, which include: identification of industrial CO_2 emitters, carbon capture (CC) operations, CO_2 liquefaction, loading and intermediate storage, transportation, unloading and receiving storage and e-MeOH production.

2.2.1. Carbon emitters

The study proposed to utilize the biogenic CO_2 for the synthesis of e-MeOH. The industries and the synthesis plants either exclusively emit biogenic CO_2 or a combination of biogenic and geogenic CO_2 during operation.

Geogenic CO_2 is emitted from industrial processes, specifically from the cement sector, where it is produced during the calcination of limestone [17]. Approximately two-thirds of total CO_2 emissions in the cement industry are geogenic emissions. The concentration of CO_2 in the flue gases from calcination ranges between 15-30% [22]. In addition to the geogenic emissions, studies indicate that biogenic sources contribute approximately 6% of total CO_2 emissions in cement plants, where the proportion of biomass relative to fossil fuels used to achieve the high temperatures required for calcination dictates the share of biogenic CO_2 emissions. Together, these sources account for nearly 72.7% of the plant's total CO_2 output [17].

Likewise, the pulp and paper industry is a major contributor to biogenic CO_2 emissions [23], accounting for approximately three-fourths of the total CO_2 emissions [24]. The pulp and paper industries release CO_2 as a component of green liquor during the combustion of black liquor or other biomass streams in the recovery boiler [24]. The underlying combustion process can be simplified as follows:

$$Fuel\ (C,\ H,\ O,\ N) + Air\ (O_2,\ N_2) \rightarrow CO_2 + H_2O + N_2 \quad (4)$$

For pulp and paper industries, literature indicates that biogenic streams typically contribute around 80% of overall emissions, while the remaining 20% originate from fossil fuels. Although the exact distribution varies among facilities [24], a comparable situation is observed in cement synthesis.

A detailed assessment of potential industrial CO_2 emitters is performed on the basis of this emission profile, to identify a potential source to supply sufficient biogenic and geogenic CO_2 for large-scale e-MeOH synthesis [22]. Although several industries emit biogenic CO_2, many are excluded due to their limited annual CO_2 emissions. Industries like biomass power plants and ethanol plants emit biogenic CO_2, but the average annual emissions of these two plants are approximately 400 and 200 kt, respectively [25]. This average annual output is significantly lower than that of cement and pulp and paper plants, making them less suitable as primary CO_2 sources. Waste-to-energy (WtE) facilities also face similar challenges. The facility emits approximately 285 kt of CO_2, among which 60% is biogenic [26]. Due to this, it also falls below the necessary threshold of this work. Similarly, alcohol and sugar production plants were also excluded due to their low CO_2 output. Only cement, pulp and paper plants are found to consistently provide the high-volume and reliable CO_2 streams for effective e-MeOH synthesis.

Both cement, pulp and paper facilities exhibit reliable emission profiles. Pulp and paper plants offer one of the largest biogenic CO_2 streams in the industrial sector. Whereas, despite the predominant geogenic emissions, the cement plant still maintains continuous geogenic CO_2 flows, with a small but well-defined biogenic component. Thus, this study specifically focuses on the cement, pulp and paper industries as the most suitable emitter for supplying geogenic and biogenic CO_2 for large-scale e-MeOH synthesis.

2.2.2. Carbon capture plant

The suitability of carbon capture technologies varies across industries due to significant differences in CO_2 concentration, pressure and flow characteristics in process off-gases and flue gases [27]. As each industrial sector produces emissions with distinct chemical compositions, this carbon capture technology must be aligned accordingly [28].

Pre-combustion capture is not compatible with cement synthesis, as most CO_2 is released during calcination instead of combustion. Though this technology performs well for fertilizer synthesis and hydrogen generation via steam methane reforming (SMR), it suffers from high sorbent regeneration energy requirements [29]. Oxy-combustion, while capable of increasing CO_2 concentration in flue gases, is excluded for cement, pulp and paper plants due to the high cost of oxygen synthesis [30,31]. Furthermore, substantial retrofitting is needed for kilns and boilers.

Amine-based post-combustion capture emerges as the most suitable option for both cement and pulp and paper industries because it efficiently handles low concentrations of CO_2 [32]. It also demands low plant modifications. Monoethanolamine (MEA) is selected as the preferred solvent, considering its maturity, despite its considerable steam demand for regeneration.

During estimating CO_2 availability, a conservative 90% capture efficiency is used and applied across scenarios to maintain modelling consistency. This value represents a widely reported and technically achievable performance level for amine-based post-combustion capture systems [33,34]. The CO_2 availability for the selected plants are shown in Table 2 [35].

Table 2
Annual compliant and available CO_2 from different industries.

Industry	Company and location	Compliant CO_2 (kt)	Available CO_2 (kt)
Paper and Pulp	Figueira da Foz, The Navigator Company (TNC)	731	658
Paper and Pulp	Aveiro, TNC	171	154
Cement	Carboneras, Holcim	1,124	1,012
Cement	Alcanar, SP, CEMEX,	1,723	1,551

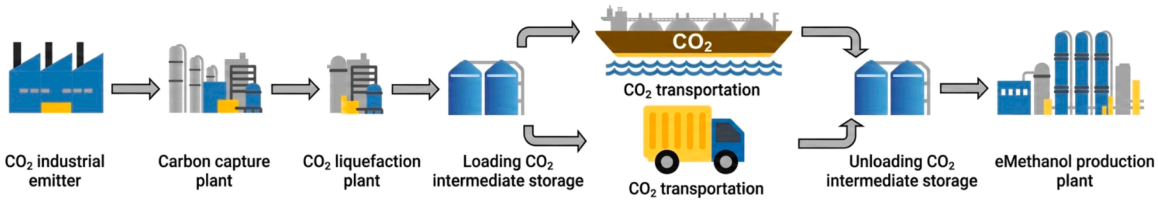

Fig. 1. Schematic of the CCU value chain modelled.

Technical sizing follows a balance-of-plant approach, assuming electric steam generation with 98% conversion efficiency and 5% steam losses. Requirements include MEA make-up flows of 0.5–3.1 t MEA/kt of CO_2, cooling water demand of 22 tonnes for each kt of CO_2 and auxiliary consumption of 75 MWh/ktCO_2. Continuous operation is based on 8497 yearly hours. The energy and mass requirements are summarized in Table 3 [29,31,32].

2.2.3. Liquefaction

The scope of this work excludes detailed sizing of individual components within the storage and liquefaction plants. Instead, the technical sizing is performed at the overall plant level to support the economic analysis, avoiding granular component-by-component assessments. The liquefaction plant design draws on the CO_2 storage hub model developed by Fraga et al. [18], which operates at 15 bar and includes a liquefaction stage positioned between the carbon capture units and intermediate storage for transport and permanent sequestration.

The CCU chain in this model is sized to manage up to 2000 kt of CO_2 per year, with an associated liquefaction energy demand of 83.1 MWh per kt of CO_2. Since the liquefaction plants operate in conjunction with amine-based post-combustion carbon capture facilities, both systems are assumed to share identical annual operating hours. Based on reported availability data, a value of 8497 operating hours per year is assumed [36].

2.2.4. Carbon transport

Transport of CO_2 is a fundamental component for maintaining operational continuity and economic viability in CCU value chains, specifically for 90–1200 kt e-MeOH synthesis systems requiring 150–2050 kt of CO_2 annually. This demand range positions the project between small to large-scale deployment, making the selection of an efficient and robust logistics strategy essential. In this study, two transport pathways, i.e., ship tankers and trucks, are evaluated as alternative or complementary solutions for delivering CO_2 from industrial emitters to an e-MeOH plant. The assessment aims to determine which mode provides the most reliable, scalable, and economically feasible option under realistic operating constraints.

Comparable large-scale experience exists in the Northern Lights project, which offers a useful reference due to its similar CO_2 throughput and its deployment of a mature shipping architecture. Northern Lights utilizes 7500 m^3 multi-gas tankers designed under LPG industry standards to reduce infrastructure modifications and accelerate fleet deployment. Operating at an approximate 15 barg and −26 to −35 °C, these vessels maintain CO_2 in its liquid state at a density of approximately 1100 kg/m^3 . With loading and unloading speeds of 800 m^3 /h and a conservative estimate of 11 h per operation, coupled with an additional 2 h for manoeuvring, the complete port cycle reaches 26 h. Accounting for regulatory survey downtime, the tankers achieve roughly 8234 operational hours annually while consuming around 11 MWh/h of fuel. These parameters inform the design of an optimized tanker fleet capable of preventing port scheduling conflicts and ensuring continuous CO_2 supply for e-MeOH synthesis [33,34,36].

On the other hand, truck-based CO_2 transport provides complementary flexibility for short-distance routes or inland. The literature shows that using 20-foot, 24 m^3 container tanks can carry up to 26.3 t of CO_2 at 15 barg. Conservative assumptions integrate an average truck speed of 80 km/h, route distances oversized by 105%, diesel consumption of 0.27 €/km and 5% downtime for refuelling and maintenance. Loading and unloading period takes 1.5 h each, and an additional 30-minute buffer ensures that multiple trucks can operate without logistical overlap, requiring several parallel loadings and unloading arms and subsystems at intermediate storage sites. According to the EU Regulation 561/2006 on driving hours, which governs the planning for logistics, imposing maximum daily driving times of 9–10 h. It leads to weekly driving hours of 56 h, followed by biweekly limits of 90 h. It is mandatory to take breaks every 4.5 h. Short routes, i.e., routes less than 4.5 h, need to integrate breaks during the loading or unloading period, whereas long routes require planned rest periods, approximately 14–15 h. To maximize utilisation, continuous operations are achieved by rotating two or three drivers per truck, depending on route duration. Trucks have a practical lifespan of approximately 5 years (1,000,000 km), whereas tank containers exceed 20 years, enabling long-term continuity and cost-efficient fleet renewal cycles [33,34,36].

Considering these assessments, both tankers and trucks offer distinct advantages depending on distance, route characteristics and operational scale. Tankers provide high-capacity, continuous transport suitable for large-scale and long-distance CO_2 transfer, while trucks offer flexibility and adaptability for shorter or inland routes. Therefore, this study aims to compare the two options under the described operational constraints for selecting the most efficient and reliable CO_2 logistics strategy for e-MeOH synthesis.

Transport operating expenditures were calculated by aggregating the major cost components associated with vehicle operation, including fuel consumption, labour, maintenance, and route-dependent charges as defined within the overall operating cost structure (Eq. 6). These annual transport costs were then included within the overall cost structure used to determine the levelized cost of CO_2 ($LCOCO_2$) according to Eq. 13.

The loading and unloading durations described above were incorporated into the estimation of the complete transport cycle time:

$$T_{loop} = T_{load} + T_{unload} + 2T_{travel} + T_{aux} \quad (5)$$

Where,

- T_{loop}: total duration of one complete transport cycle (h)
- T_{load}: time required to load CO_2 into the transport unit (h)
- T_{unload}: time required to unload CO_2 at the destination (h)
- T_{travel}: one-way travel time between source and destination (h), determined from route distance and transport speed
- T_{aux}: additional operational time required for handling, manoeuvring, or buffering operations depending on the transport mode (h)

$$OPEX_{transport} = C_{fuel} + C_{labour} + C_{maintenance} + C_{mode} + C_{tax} \quad (6)$$

Where,

- $OPEX_{transport}$: total annual operating cost associated with CO_2 transport
- C_{fuel}: annual fuel or diesel consumption cost
- C_{labour}: annual driver or crew cost
- $C_{maintenance}$: annual maintenance cost of trucks or vessels
- C_{mode}: transport-mode-specific cost component, including harbour fees for tanker transport or toll fees for truck transport
- C_{tax}: annual vehicle or regulatory tax costs

2.2.5. Intermediate carbon storage

The assessment of CO_2 storage tanks is based on the intermediate CO_2 storage system of the Northern Light project. The reference tanks are vertically oriented. The pressurized units have 6.1 m diameter, 35 m of height and 21.8 barg of pressure. The operating temperature is approximately -46 to 50 °C. In this study, operating conditions of 13–18 barg and −30.8 to 20.8 °C temperature is considered for the analysis. This assumption is aligned with the broader transport–storage value chain. The terminal comprises 12 storage tanks, each with a

Table 3
Technical specifications for capturing a kt of CO_2 per year.

Resource	Annual consumption	Unit (per year)
Amine-MEA make-up	0.003	kt
Water for cooling	0.022	kt
Auxiliary electric consumption	75	MWh
Electric reboiler	888	MWh

capacity of approximately 760 m^3. Of this, 625 m^3 accommodates the CO_2 volume delivered by a 7500 m^3 ship, leaving the remaining 22% as overcapacity. Because the logistics model employs mass units, the mass of CO_2 transported varies according to density at the selected pressure and temperature.

The overall storage system is designed to support 1.5 Mt per year of CO_2 transported by ship. Assuming linearity, each tank corresponds to approximately 125 kt of CO_2 throughput. Therefore, total storage capacity must be installed in increments of 7500 m^3 to accommodate full tanker offloading. At the selected 15 barg storage pressure, the gravimetric site capacity is 10,044 t, with 9056 t available operationally. The system is designed for a 25-year lifetime.

Loading and unloading systems, comprising loading arms, pipelines, pumps, heaters, coolers, compressors and valves, are treated as an integrated system sized for the full annual CO_2 capacity. No optimization is applied when tankers are included, consistent with Northern Lights' design philosophy. Equipment is assumed to have a minimum 25-year lifetime, with 8716 annual operating hours and 0.5% unavailability. Finally, loading and unloading systems are considered technically equivalent, as both must accommodate identical CO_2 flows when transport losses are neglected.

2.2.6. E-MeOH synthesis plant

This study designs an e-MeOH plant through a simplified balance-of-plant methodology. This modelling approach followed a similar design process to the carbon capture plant. The approach concentrates on the key electricity-consuming units and their associated mass requirements to determine the levelized cost of e-MeOH (LCOeM). While conventional MeOH plants particularly rely on fossil or biomass combustion to supply reboiler heat, this study considers an electric boiler. It also ensures methodological consistency with the carbon capture plant and supports full electrification. The electric boiler is assumed to operate with a conversion efficiency of 98%. An additional 5% thermal loss is included to account for steam system losses during heat distribution and operation. For more accurate and clear modelling, the study includes hydrogen feedstock, CO_2 feedstock and cooling water as a mass. The electric energy requirements comprise compression of H_2 and CO_2 feedstocks, compression for recirculation, including pressure-drop compensation and electricity for providing distillation heat through the electric boiler. The applied values originate from averaged data reported in different studies simulating e-MeOH or conventional MeOH plants. These values are summarised in Table 4, which provides the annual mass and electricity demands per 1 kt of installed e-MeOH capacity [29,31,32].

The operational expenditure (OPEX) drivers relevant to e-MeOH synthesis are consequently identified and quantified in this study. Furthermore, the catalyst consumption rates range from 92.7-101.1 kg per kt of e-MeOH [29,31,32]. Accordingly, it is assumed that the average catalyst consumption is 96.9 kg/year/kt to produce e-MeOH. Finally, based on literature [18], the plant is modelled with a 20-year operational lifetime and 8090 annual operating hours, consistent with typical industrial practice and with published simulations [30].

Table 4
Mass and required electricity demand per 1 kt of installed e-MeOH capacity.

Magnitude	Quantity	Unit (year)
H_2	0.2	kt
CO_2	1.5	kt
Catalyst	0.1	t
H_2O for cooling	4.8	kt
Compression H_2	70	MWh
Compression CO_2	99	MWh
Compression recirculation	69	MWh
Electric Reboiler	448	MWh

2.3. Assessment criteria

According to the objective of this study, the research aims to develop integrated calculations for each stage of the process and combine their results to determine the total cost for a selected pathway to produce e-MeOH. In this study, the LCOeM is estimated. For this purpose, the LCOeM is broken down into different stages through the levelized cost of carbon dioxide ($LCOCO_2$).

The levelized cost of energy (LCOE) is the unit cost of energy produced throughout the economic life of a project. There are two primary methods present to calculate the levelized cost, i.e., the annuitizing method and the discounting method. The annuitizing method is developed by the US National Renewable Energy Laboratory (NREL) [37], whereas the discounting method is proposed by the UK Government Department for Business, Energy & Industrial Strategy (BEIS) [38]. This study considered the BEIS method due to its comprehensive approach with an upfront approach for the fuel and the capital costs.

The LCOeM adopts the LCOE metric and is calculated by using Eq. 7.

$$LCOeM = \frac{PLC}{LP_{eMeOH}} = \frac{€}{kt\ eMeOH} \tag{7}$$

The PLC denotes the Project Lifecycle Cost in euros (€) and the $LP_{e\text{-}MeOH}$ denotes the Lifetime Production of e-MeOH in kt. The PLCs are typically categorized into four main types, i.e., development expenditure (DEVEX), capital expenditure (CAPEX), OPEX and decommissioning or site restoration expenditure.

DEVEX includes the early project development costs, starting from initial planning to the Final Investment Decision (FID). These costs incorporate feasibility assessments, permitting activities and early engineering work. CAPEX covers the expenses required to construct and commission the facility, while OPEX represents the recurring costs of operating it. This includes materials, labour, maintenance and utilities. Decommissioning costs arise at the end of the asset's life for dismantling and site restoration. In this study, only CAPEX and OPEX are considered in the levelized cost analysis, excluding DEVEX, decommissioning costs. The study also assumed OPEX to be constant to simplify the evaluation and align with common practices.

The study evaluated both costs and synthesis volumes in Net Present Value (NPV) terms. It ensures the future expenditure and outputs are appropriately discounted to their present value for accurate comparison with recent economic output. NPV is estimated as Eq. 8.

$$LCOeM = \frac{NPV_{Cost}}{NPV_{eMeOH}} = \frac{\sum_{t=1}^{N} \frac{CAPEX_t + OPEX_t}{(1+d)^t}}{\sum_{t=1}^{N} \frac{eMeOH\ capacity_t}{(1+d)^t}} \tag{8}$$

Where N is the plant operating lifetime in years, t is the specific year, i is the inflation rate and d is the discount rate. In this study, nominal discount rate and inflation rate are considered to be 2.21% and 8%, respectively [21]. The study used Eq. 9 to calculate the real discount rate, which is approximately 5.66%.

$$d = \frac{1 + d_n}{1 + i} - 1 \tag{9}$$

If the discount rate is similar to the Internal Rate of Return (IRR), then the NPV of the project is zero. Therefore, based on this, the LCOeM is estimated as Eq. 10.

$$NPV_{project} = NPV_{revenues} - NPV_{costs} = 0 \tag{10}$$

$$LCOeM = \frac{NPV_{revenues}}{NPV_{eMeOH\ capacity}} \tag{11}$$

In this study, this LCOeM can be segmented into different stages as shown in Eq. 12.

$$LCOeM = LCOCO_{2\ Capture} + LCOCO_{2\ Liquefaction} + LCOCO_{2\ Loading\ intermediate\ storage} + LCOeM_{CO_2\ Transport} + LCOCO_{2\ Unloading\ intermediate\ storage} + LCOe\text{-}MeOH_{Production} \quad (12)$$

Where $LCOCO_{2\ Capture}$ is the capturing cost of CO_2 from the source, $LCOCO_{2\ Liquefaction}$ is the liquefying cost of CO_2 throughput from the carbon capture plant, $LCOCO_{2\ transport}$ is the liquid CO_2 transport cost, $LCOCO_{2\ loading\ intermediate\ storage}$ and $LCOCO_{2\ unloading\ intermediate\ storage}$ are the liquid CO_2 loading and unloading costs, respectively, $LCOe\text{-}MeOH_{production}$ is the e-MeOH synthesis cost that includes H_2 and CO_2 feedstock acquiring cost.

The $LCOCO_2$ for each step is evaluated by Eq. 13.

$$LCOCO_2 = \frac{Total\ annualized\ CAPEX + OPEX}{Annual\ CO_2\ supplied\ or\ processed \quad (t\ per\ year)} = \frac{I_t + O_t}{\frac{CO_{2,\ t}}{(1+r)^t}} \quad (13)$$

Where I_t is the CAPEX in year t, O_t is the OPEX in year t, $CO_{2,\ t}$ is the amount of CO_2 supplied or processed in this year, r and t are the discount rate year Index.

The CAPEX is estimated by Eq. 14.

$$CAPEX_1 = CAPEX_2 \left(\frac{C_1}{C_2}\right)^{\alpha} \quad (14)$$

Where $CAPEX_2$ and $CAPEX_1$ are the capital costs at the desired capacity level of C_2 and C_1, respectively. This equation follows the power-law scaling relationship with α=0.6 and is known as the 0.6 rule.

In a real scenario, the actual CO_2 handled is less than the theoretical maximum due to downtime, maintenance or inefficiencies.

The actual CO_2 is estimated by Eq. 15.

$$CO_{2,t}^{actual} = CO_{2,t}^{max} \times AF \quad (15)$$

The AF is the annualized factor or the capacity factor. It is estimated by Eq. 16.

$$AF = \frac{Actual\ CO_2\ handled\ or\ plant\ running\ time}{Theoritical\ maximum\ CO_2\ handling\ if\ plant\ run\ for \quad 24/7} = \frac{(1+r)^n - 1}{r(1+r)^n} \quad (16)$$

Where r and n are the discount rate and project lifetime in years.

This study assumed for simplicity that CAPEX for all assets within the project's value chain is incurred entirely in the year prior to the start of operations, even though acquisition timelines may differ and could realistically span more or less than a single year.

2.4. Scenario selection and techno-economic specifications

To select the scenarios for simulation, it is essential to establish industrial cases that are both realistic and technically feasible. The study focuses on the availability of biogenic and geogenic CO_2 for e-MeOH synthesis. This work proposes to compare two different transport modes, i.e., tanker and truck, in this CCU value chain. Thus, it is essential that eligible CO_2-emitting industries are located within 15 km of a port equipped with liquid cargo infrastructure, eliminating the need to model CO_2 transport between the emission source and the harbour. Within the Iberian Peninsula, selected as the geographical area for this study, the major ports include Algeciras, Aveiro, Barcelona, Bilbao, Lisbon, Sines, Tarragona, and Valencia.

A systematic selection method is applied to identify eligible CO_2 sources for the targeted scale e-MeOH synthesis. The initial dataset includes all industrial CO_2 emitters in Spain and Portugal. While all targeted industrial sectors, specifically cement, pulp and paper, are present across both countries, plant size emerged as a key determinant. Small-scale emitters are excluded to ensure sufficient feedstock availability. Existing literature shows that large European cement and pulp and paper plants operate within a total yearly CO_2 emission range of 600–740 kt, but the share of renewable fuels of Non-Biological origin (RFBNO)-compliant emissions varies by sector. It is observed that cement industries emit approximately 66.7% of geogenic CO_2, i.e., two-thirds of total emissions, while biogenic emissions contribute around 6% in RFBNO-compliant CO_2. Whereas in Pulp and Paper manufacturing, both process-related emissions and emissions from biomass combustion are biogenic, making roughly 80% of total plant emissions RFBNO-compliant. These distinctions are incorporated into the selection process to ensure accurate feedstock estimation.

To quantify the CO_2 available for e-MeOH synthesis, sector-specific emissions factors are applied, 0.595 t of CO_2 per ton product for cement and 0.667 t of CO_2 per ton for the pulp and paper industry [39, 40]. The selection result shows that Iberian plants provide an average of 1032 kt of CO_2, which is above the typical European average. Furthermore, the CIMPOR Alhandra cement site stands out with a capacity of 2248 kt. Therefore, all selected scenarios represent large-scale, high-potential emitters suitable for CCU integration.

The selected five scenarios are defined, each linking one industrial CO_2 resource to the e-MeOH plant (which is assumed to be located at the Port of Sines, Portugal) via tanker or truck. The selected scenarios are shown in Table 5 with a detailed dataset [41,42]. The annual CO_2 available at the considered industrial emitter and the corresponding e-MeOH production is listed in Table 6. The distance of the route with different transport mediums in km are also included in this table.

The other techno-economic specifications of this overall value chain for estimating the levelized cost of e-MeOH are discussed in Table 7 [7, 17–19,43,44–54]. This study excluded the pipeline required for transporting CO_2 from the e-MeOH plant to the receiving intermediate storage site. Similarly, this exclusion applies to interconnections between the carbon capture plant and the liquefaction plant, as well as between the liquefaction plant and the origin intermediate storage site.

The relatively high reported CCU-related cost components arise primarily from conservative system configuration and boundary assumptions. The process design adopts electrically driven steam generation for solvent regeneration and applies fixed energy requirements without explicit heat integration or process optimization. These modelling choices are intended to provide consistent performance estimates but may result in higher levelized costs compared with highly optimized or site-specific integrated systems reported in the literature.

2.5. Methodology

To estimate the cost, the analysis begins by identifying and characterizing potential industrial CO_2 sources capable of supplying the required feedstock for e-MeOH synthesis. Based on these sources, techno-economic specifications of the carbon capture plant are established to define capture performance and cost parameters. Subsequent steps assess the feasibility and design of a CO_2 liquefaction unit, followed by the evaluation of an intermediate storage facility to enable efficient loading for transport. Logistics optimization is then carried out for the transportation stage, focusing particularly on the configuration and sizing of a truck and tanker fleet capable of reliably meeting the plant's CO_2 demand. After transport, the receiving intermediate storage system at the e-MeOH site is analysed and dimensioned to ensure an uninterrupted CO_2 supply during operation. Finally, the e-MeOH plant itself is sized to determine its precise CO_2 consumption rate. This final step establishes the required CO_2 throughput for the entire supply chain and directly links upstream supply design to the targeted e-MeOH synthesis capacity.

The techno-economic parameters applied in this study represent base-case assumptions rather than worst-case conditions. Standard engineering relationships, including the use of a CAPEX scaling exponent ($\alpha = 0.6$), are adopted to approximate typical industrial cost behaviour, consistent with established cost estimation practices and commonly

Table 5
Capacity, production and emission factor for all the scenarios [41,42].

Scenario	Origin	Industry	Company	Total production capacity per year (Mt)	Emission factor	Total CO_2 capacity per year (kt)	RFBNO-compliant CO_2 per year (kt)
Scenario 1	Figueira da Foz	Paper and Pulp	TNC	1,370	0.667	914	731
Scenario 2	Aveiro	Paper and Pulp	TNC	320	0.667	213	171
Scenario 3	Carboneras	Cement	Holcim	2,600	0.595	1,547	1,124
Scenario 4	Alcanar	Cement	CEMEX	3,985	0.595	2,371	1,723

Table 6
Transport distances and e-MeOH synthesis capacities for the selected scenarios.

Scenario	Industry	Company and Origin	Distance (km)		Available CO_2 per year (kt)	e-MeOH synthesis capacity CO_2 per year (kt)
			Truck	Tanker		
Scenario 1	Paper and Pulp	TNC, Figueira, PT	360	321	658	390
Scenario 2	Paper and Pulp	TNC, Aveiro	438	400	154	90
Scenario 3	Cement	Holcim, Carboneras	836	878	1,012	600
Scenario 4	Cement	CEMEX, Alcanar	1,250	1,203	1,551	920

applied ranges reported in techno-economic assessments of CCU systems [31,55].

2.5.1. Sensitivity analysis

The sensitivity analysis is conducted by varying hydrogen prices across three scenarios (2, 6, and 8 €/kg) while keeping all other input parameters constant. For each price level, LCOeM and $LCOCO_2$ are recalculated for all scenarios and transport modes. This approach isolates the impact of hydrogen cost on overall system economics. The results enable comparison of cost responsiveness and identification of the most economically robust transport configurations.

3. Results and discussions

The following section presents and discusses the LCOeM and $LCOCO_2$ results obtained for the four defined scenarios. The results are based on the integrated CCU value chain model. These results compare different industrial CO_2 emitters, supply characteristics and transport mode and identify the most influential factors that affect the overall economics of e-MeOH synthesis. The LCOeM and $LCOCO_2$ values derived from each scenario are also discussed below.

3.1. Levelized cost of e-MeOH simulation

The levelized costs for e-MeOH of different scenarios under two separate transport modes are shown in Fig. 2.

Fig. 2 reports the LCOeM for four scenarios, comparing CO_2 delivery by truck with respect to tanker. The results fall in a relatively narrow band (approximately 1102–1278 €/t e-MeOH). This indicates that while CO_2 delivery affects the total cost, large parts of LCOeM are driven by upstream conditions, e-MeOH synthesis and plant economics, specifically hydrogen supply and power price assumptions.

A key insight is the interaction between CO_2 throughput and logistics distance. Scenario 2 shows the highest LCOeM, which is about 1.25–1.25 k€/t, despite not having the longest route. This is because the available CO_2 is comparatively low (154 kt), which limits the e-MeOH synthesis capacity at 90 kt and reduces utilization of fixed capital assets across the chain. This includes capture, liquefaction, intermediate storage and loading/unloading infrastructure. In such low-throughput cases, cost components that scale weakly with flow become dominant, pushing up the levelized cost even when transport distances are moderate.

Scenario 1 achieves the lowest levelized cost for both the transport modes because of shorter transport distance and comparatively higher CO_2 availability of 658 kt. This enables better utilization of logistics assets and downstream synthesis capacity. This result highlights that viable CO_2 sources for e-MeOH are not only those with favourable emissions factors, but also those that can deliver stable, high-volume CO_2 streams that pay off fixed costs.

For the cement-based scenarios (scenarios 3 and 4), the levelized cost is lower than that of scenario 1 for the tanker-based transport mode. Even for truck transport, the LCOeM of these scenarios are close to scenario 1. This suggests that larger CO_2 availability and higher potential e-MeOH synthesis volumes partially offset the distance penalty through scale effects. This indicates that longer routes can be economically feasible when they reveal larger, more concentrated industrial CO_2 streams that improve utilization of capture, liquefaction, and storage systems. However, under current EU RFNBO regulations, industrial CO_2 sources such as cement plants are permitted only as transitional sources until 2041, after which stricter eligibility criteria are expected to limit the use of non-compliant stream [56]. Consequently, the effective availability of RFNBO-compliant CO_2 from cement facilities would decline substantially, which would reduce achievable e-MeOH synthesis capacity and consequently increase the resulting LCOeM.

Transport mode effects are scenario -dependent. Tanker and truck outcomes differ modestly in scenarios 1 and 2, implying that in shorter-to-moderate corridors, the total LCOeM is less sensitive to the transport mode and more governed by the broader economic structure. However, the gap widens in longer-distance cases, where tanker transport becomes relatively more competitive. This is consistent with higher payload and better tkm efficiency of maritime transport. This can reduce variable logistics cost per unit CO_2 delivered when distances are high, and volumes are sufficient to utilize vessel capacity.

Overall, the result highlights that optimal levelized cost is both scale and distance-aware. High throughput, long-distance corridors support maritime solutions, while decentralized or moderate-scale facilities support flexible road transport. To better interpret these scenario-dependent variations, the overall LCOeM must be decomposed into its constituent process steps, revealing the relative contribution of capture, conditioning, transport, storage, and synthesis.

The stage-wise averages summarized in Table 8 clarify the structural origin of LCOeM differences between tanker and truck transport. In both configurations, the dominant contribution arises from the methanol synthesis, which remains identical at 960.63 €/t and accounts for approximately four-fifths of the total costs. This indicates that hydrogen supply, electricity consumption and synthesis CAPEX are the primary cost drivers of the overall system. Carbon capture represents the second

Table 7
Techno-economic specifications for estimating the levelized cost of e-MeOH.

Category / Component	Parameter / Criterion	Value / Assumption / Equation*	References **
General Economic Assumptions	Base year	2024	[7,17,18]
	Discount rate	8%	
	Inflation	2.21%	
	Project lifetime	20	
	Electricity price	40 €/MWh	
CO_2 Capture (MEA Post-combustion)	CO_2 concentration	Cement: 20–25% vol; Pulp/Paper: 12–14% vol	[19,43–46]
	Capture efficiency	90%	
	CO_2 purity output	98–99%	
	Compression energy	150 kWh/tCO_2	
	CAPEX	200,850 €/ktCO_2	
	MEA makeup	1.77 €/kg	
	Cooling water	0.051 €/m³	
	Process water	0.243 €/m³	
Liquefaction	Electric consumption	100–130 kWh/tCO_2	[44,45,47]
	CAPEX ratio	21,319 €/ktCO_2	
	OPEX	10% of CAPEX	
Truck Transport	Truck + ISO tank CAPEX	260,000 €	[45,48–51]
	Payload	26.3 tCO_2/trip	
	Diesel price	1.668 €/L	
	Driver cost	24.8 €/h	
	Maintenance	0.138 €/km	
	CO_2 tax	100.57 €/yr	
	Vehicle tax	390.08 €/yr	
	Toll fees	Route-dependent	
Tanker Transport	Vessel CAPEX	8,164 €/m³	[18,44]
	Cargo tank capacity	7,500 m³	
	Fuel cost	49.77 €/MWh	
	Fuel consumption	12,729 €/day	
	Crew size / cost	20 people / 772,339 €/yr	
	Harbour fee	11,446 €	
	Maintenance	2% of CAPEX	
Intermediate CO_2 Storage	Tank farm CAPEX	2,506 €/m³	
	Capacity	9,150 m³	
	Residence time	2–3 days	
	Loading/ unloading system CAPEX	1,977 €/tCO_2/yr	
	Tank farm OPEX	7% of tank farm CAPEX	
	Loading/ unloading system OPEX	3% of loading/ unloading system CAPEX	
E-MeOH Plant	CAPEX (per year)	554,537 €/kt (avg.)	[51,52]
	Reference plant (per year)	440 kt; 277,965,651 €	
	H_2 price	4 €/kg	
	Catalyst price	35.62 €/kg	
	Stoichiometry	$CO_2 + 3H_2 \rightarrow CH_3OH + H_2O$	
	H_2 consumption	0.19 t H_2 / t MeOH	
	CO_2 consumption	1.375 tCO_2 / t MeOH	
	Conversion efficiency	70–75%	
	Heat integration	Assumed, reduces net energy by 8–12%	
CO_2 Acquisition & Market Assumptions	CO_2 feedstock cost	100 €/tCO_2	[51–53]
	EUA price	55–105 €/tCO_2	
	EUA forecast	83–149 €/tCO_2	

* Parameter ranges are reported as given in the cited sources for traceability. For model calculations, the average value within each reported range was used.
** Some data were gathered through personal communications with industry experts.

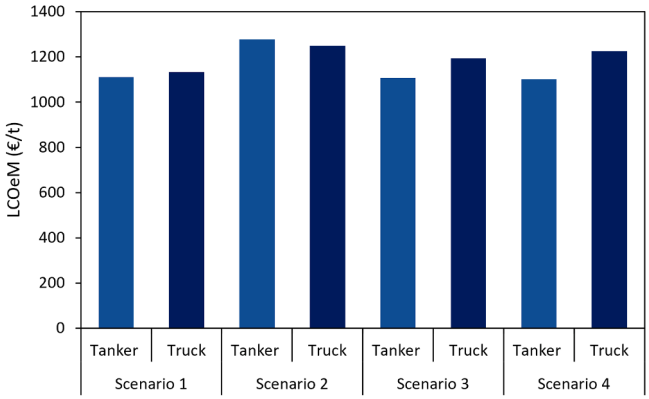

Fig. 2. LCOeM for different scenarios.

Table 8
Comparison of the averaged levelized costs.

Component	Average per stage for Tanker	Average per stage for Truck
Synthesis	960.6	960.6
Transport	46.9	99.3
Storage	29.9	29.9
Liquefaction	11.9	11.7
Capture	100.3	99.3
LCOeM	1149.6 €/t e-MeOH	1200.8 €/t e-MeOH

largest share, while liquefaction and storage contribute comparatively minor increments, suggesting limited sensitivity of the total LCOeM to improvements in these conditioning stages. The principal divergence between the two pathways is observed in the transport cost, which increases from 46.9 €/t for tanker delivery to 99.3 €/t for truck delivery, approximately twice. This results in a corresponding increase in total LCOeM from 1149.7 to 1200.8 €/t e-MeOH. The analysis demonstrates that, although logistics is not the largest absolute contributor, it is the most influential variable component distinguishing the scenarios, with marine transport benefiting from higher payloads and lower specific tkm costs.

The overall assessment indicates that Scenario 4 is economically favourable when CO_2 is transported by tanker. In contrast, truck transport for the same scenario results in significantly higher costs as compared with the other scenarios. To better understand these differences, the contribution of each process stage to the total levelized cost is further analysed, as illustrated in Fig. 3.

Fig. 3 compares the stage-wise LCOeM for scenario 1 under tanker and truck transport modes, clearly indicating the influence of logistics on overall system economy. Tanker transport yields a lower LCOeM of 1111.3 €/t e-MeOH, whereas truck delivery increases the cost to 1133.5 €/t, representing an increment of more than 2.3%. While the synthesis stage remains the dominant contributor in both cases, the transport component exhibits the largest deviation, rising from 24.4 €/t for tanker to 47.7 €/t for truck, reflecting the higher specific tkm costs and reduced payload efficiency of road-based logistics. In contrast, capture, liquefaction and storage costs remain nearly unchanged, indicating that the observed economic gap is primarily driven by transport-related expenditures rather than upstream processing. These findings justify the preference for tanker-based CO_2 delivery in long-distance, high-volume scenarios and demonstrate the strong sensitivity of LCOeM to logistics choices. Therefore, a dedicated levelized cost of CO_2 assessment is necessary to isolate and quantify the contribution of each conditioning and transport stage within the value chain.

3.2. Levelized cost of carbon di-oxide analysis

The study simultaneously assessed the levelized cost of CO_2 by

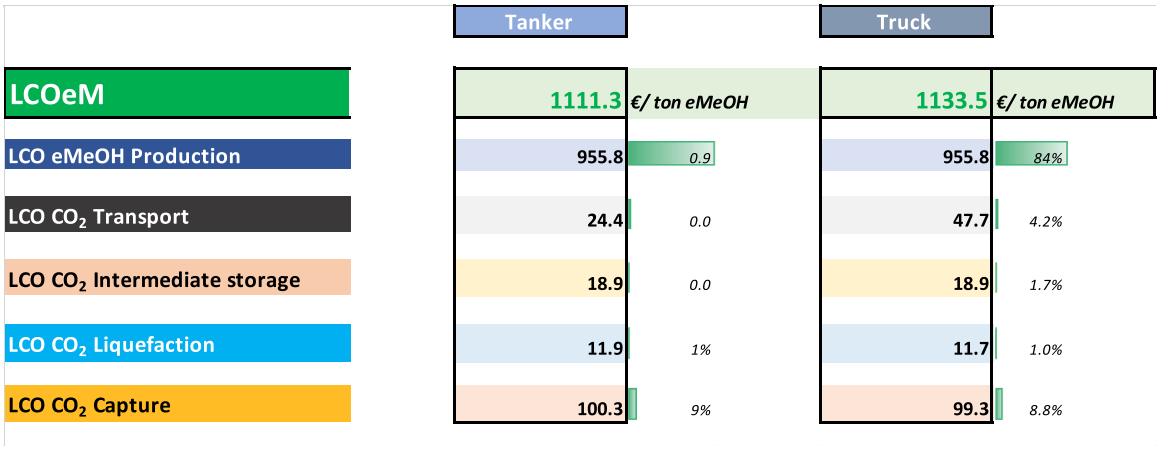

Fig. 3. LCOeM for scenario 1 under different transport modes.

excluding e-MeOH synthesis stage from the CCU value chain model. This $LCOCO_2$ is evaluated for the stages of carbon capture, loading and unloading intermediate storage, liquefaction and transport.

3.2.1. *Maritime and road transport*

The $LCOCO_2$ results for each of the CCU value chain stages under two different transport modes are shown in Fig. 4.

The figure illustrates the relative contributions of transport, storage, liquefaction, and capture to the $LCOCO_2$ across four transport scenarios, each evaluated for tanker and truck modes. The exact numerical breakdown of each component is provided in Table 9.

Across all configurations, capture constitutes the dominant and nearly constant cost component, remaining around 65 €/t, and therefore establishes a consistent baseline contribution to total system cost. Similarly, liquefaction varies only marginally, indicating that these two stages contribute little to cost differentiation among scenarios. As a result, the variability in total $LCOCO_2$ observed in the stacked bars is primarily governed by changes in transport and storage costs rather than processing operations. The minor decimal differences reported in Table 9 arise from the different annual operating hours considered for tanker and truck fleets. Due to longer maintenance-related downtime, tanker operation presents lower effective utilisation, which in turn affects the amount of CO_2 handled across the linked value-chain stages, resulting in slight variations in the corresponding unit costs visible only at thesecond or third decimal place.

Storage costs show notable scenario dependence, with scenario 2 exhibiting substantially higher values (52.1 €/t for both tanker and truck) compared to scenarios 1, 3, and 4, where storage ranges from 5.5 to 12.4 €/t. This elevated storage cost significantly increases the overall costs of scenario 2, contributing to the highest tanker total (181.9 €/t) and a comparably high truck total (163.3 €/t). This outcome is driven by the assumption of fixed storage capacity across scenarios. As a result, the lower CO_2 throughput in scenario 2 limits the benefits of economies of scale and increases the unit cost of intermediate storage. In contrast, the relatively high CO_2 throughput of the other scenarios moderate their total $LCOCO_2$ even when transport costs increase. These findings indicate that intermediate storage can strongly influence overall economic performance and should be considered alongside transport decisions.

Transport, however, remains the most influential and variable cost driver between modes. Tanker transport costs range from 16 to 56.4 €/t, resulting in comparatively moderate totals of 101.8, 181.9, 104.5, and 106.5 €/t across the four scenarios. Truck transport exhibits much greater dispersion, increasing from 31.2 to as high as 109.1 €/t, which correspondingly elevates total $LCOCO_2$ to 116.3, 163.3, 161.7 and 187.4 €/t. Particularly for scenarios 3 and 4, the sharp rise in road transport costs produces substantial increases in total system cost, as reflected by

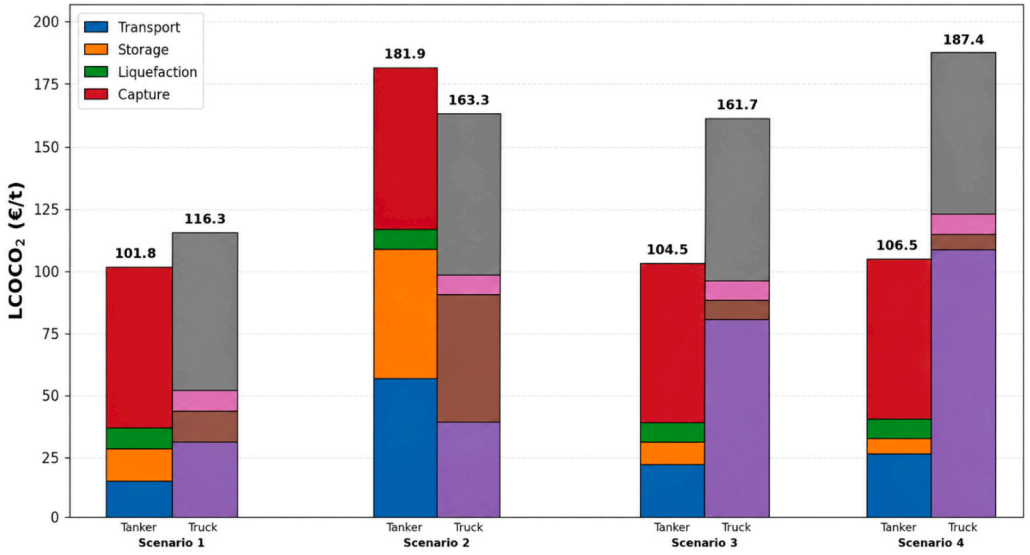

Fig. 4. $LCOCO_2$ with different transport under different unit.

Table 9
$LCOCO_2$ breakdown by value-chain stage across scenarios.

	Scenario 1		Scenario 2		Scenario 3		Scenario 4	
	Tanker	Truck	Tanker	Truck	Tanker	Truck	Tanker	Truck
Transport	16	31.2	56.4	38.8	22.8	80.7	27.6	109.1
Storage	12.4	12.4	52.1	52.1	8.2	8.2	5.5	5.5
Liquefaction	7.8	7.7	7.8	7.7	7.8	7.7	7.8	7.7
Capture	65.6	65	65.6	65	65.6	65	65.6	65
$LCOCO_2$ (€/t)	101.8	116.3	181.9	163.3	104.5	161.7	106.5	187.4

the noticeably taller stacked bars. Overall, tanker-based transport demonstrates lower and more stable cost performance, while road transport introduces greater sensitivity to route length and logistical constraints. These results suggest that optimization of transport mode selection offers the most effective pathway for minimizing total CO_2 management costs.

The cost breakdown reported in Table 9 further substantiates the trends observed in the figure by quantifying the relative contribution of each process step to the overall $LCOCO_2$. Capture consistently dominates the cost structure, accounting for roughly 35–65% of total cost depending on the scenario and transport mode, with the highest shares observed where transport and storage costs are low. Liquefaction contributes only a minor fraction (typically below 8%), confirming its limited influence on overall variability. In contrast, transport exhibits the largest proportional fluctuations, representing less than 20% of total cost for some tanker cases but increasing to more than half of the total in long-distance or truck-based scenarios, thereby driving the pronounced rise in system cost. Storage costs also become significant in specific scenarios, where it can approach one-third of the overall expenditure and substantially elevate totals even when transport remains moderate. Collectively, these proportional differences indicate that while processing costs remain relatively stable, logistical factors–particularly transport mode and scenario-dependent storage cost govern most of the economic divergence between scenarios, reinforcing the importance of transport mode selection based on transport distance and CO_2 throughput to achieve lower overall CO_2 management costs. The overall assessment demonstrates that the economies of scale, driven by CO_2 availability and industry type, have strong influence on the levelized cost distribution. Though transport distance plays a secondary role, it has a meaningful impact. Scenarios with high CO_2 supply and moderate distance perform better than others.

Building on the scenario-specific and percentage-based comparisons discussed above, the averaged values are presented to consolidate these route-level variations into a representative mode-wise cost structure. Table 10 provides an average analysis and thereby smoothing individual fluctuations and enabling a clearer assessment of the contribution of each stage to the overall $LCOCO_2$ for maritime and road transport systems.

The averaged results confirm that capture remains the dominant cost element for both transport modes, contributing more than half of the total cost under maritime conditions and slightly over two-fifths under road transport. In contrast, liquefaction exhibits the smallest contribution in both cases, accounting for less than 7% of the total, reinforcing its minimal influence on overall economic variability. Storage shows a moderate and nearly identical absolute contribution for both modes, though its relative share is slightly reduced for road transport. These observations indicate that processing-related costs remain comparatively stable regardless of the selected transport pathway.

Table 10
Average $LCOCO_2$ for each stage.

Stages	Average cost under maritime transport (€/t of CO_2)	Contribution in (%)	Average cost under road transport (€/t of CO_2)	Contribution in (%)
Transport	30.7	24.8	64.9	41.3
Storage	19.5	15.8	19.5	12.4
Liquefaction	7.8	6.31	7.7	4.9
Capture	65.6	53.1	65	41.3
$LCOCO_2$	123.6		157.2	

The primary distinction between the two modes arises from transport expenditure, which increases substantially under road-based systems and becomes the largest proportional contributor, exceeding two-fifths of the total $LCOCO_2$. Under maritime transport, however, the transport share remains considerably lower, accounting for approximately one-quarter of the total cost. This marked difference explains the higher overall average $LCOCO_2$ observed for road transport compared with maritime alternatives. Collectively, the results emphasize that while capture establishes a consistent baseline cost, logistical considerations, particularly the choice of transport mode govern the overall economic performance, further supporting the preference for maritime transport as a more cost-effective option for large-scale CO_2 movement.

Overall, the integrated analysis demonstrates that the economics of the CCU value chain are governed primarily by scale-dependent production and capture costs, while transport logistics act as the key differentiating factor between pathways. Maritime transport consistently offers lower and more stable costs for high-volume, long-distance corridors, whereas road transport becomes progressively less competitive as distance and throughput increase. These findings underscore the importance of aligning CO_2 source selection, infrastructure planning, and transport mode with system scale to achieve minimum levelized costs and maximize the economic viability of e-MeOH synthesis.

A benchmarking comparison with recent literature is added using current 2024–2026 studies that are directly relevant to renewable methanol and CO_2-based fuel supply chains (see Table 11). The selected studies represent different geographic regions, scales of deployment, and energy system assumptions. These parameters are explicitly included in Table 11 to highlight how cost variations arise from location-specific factors such as renewable resource availability, hydrogen price and infrastructure scale. This enables a consistent interpretation of the present results relative to both European and global benchmarks.

The LCOeM values obtained in this study (1111.3–1278 €/t) fall within the range of reported European studies, though generally toward the upper bound. This is consistent with industrial-scale assessments such as Omar and Widgren [41] and Hank et al. [42], where costs remain high due to strong dependence on hydrogen and electricity prices. In contrast, studies considering favourable trade conditions, such as Galimova et al. [36] and reports by the International Renewable Energy Agency [42], indicate lower cost ranges, highlighting the influence of access to low-cost renewable energy and advantageous geographic conditions. For the CO_2 value chain, the $LCOCO_2$ values in this work (101.8–187.4 €/t) are higher than those reported in large-scale CCUS projects in China, such as Liu et al. [44], where costs are reduced due to short transport distances, pipeline-based systems, and integration with EOR.

These differences underline that cost variations are primarily driven by geography, scale and energy prices. In particular, European cases typically involve higher electricity and hydrogen costs and more

Table 11
Cost benchmark against selected literature

Reference / Project	Region	System / Scope	Reported Cost Range	Key Notes
This proposed work	Iberia (Spain–Portugal, EU)	Integrated CO_2-to-e-methanol (capture + liquefaction + storage + transport + synthesis)	LCOeM: 1111.3–1278 €/t $LCOCO_2$: 101.8–187.4 €/t	Full-chain modelling including logistics and operational constraints
Galimova et al., 2025 [36]	Spain	National-scale supply chains	614–1072 €/t e-MeOH	Geography and trade strongly influence cost
Omar and Widgren, 2024 [41]	Sweden	Industrial scale	1394 €/t e-MeOH	H_2: 5.72 €/kg; H_2 contributes 60% of cost
IRENA Renewable Methanol, 2021 [57]	Global	Techno-economic outlook	~800–1600 USD/t e-MeOH	H_2 dominates cost
Hank et al., 2018 [42]	Germany	Industrial scale	608–1453 €/t e-MeOH 1028–1067 €/t 1200–2400 USD/t	Electricity & H_2 cost dominant
Lin et al., 2026 [58]	China	1358 t of methanol	823–1020 US$/t	Water electrolysis and wind farm dominates the cost
Liu et al., 2022 [43]	China	Capture + transport + EOR	~15–20 €/tCO_2 Transport: 10–30 €/t /100 km Storage: 5–15 €/t	Short distance (30–100 km)

complex logistics, while Asian systems often benefit from integrated infrastructure and lower operational costs. Therefore, the results of this study are consistent with the literature when these contextual factors are considered. Importantly, the contribution of this work lies in its integrated methodological framework, which explicitly incorporates CO_2 supply chain, e-MeOH production, and their associated operational constraints, and the presented case should be interpreted as location-specific, with results expected to vary under different regional conditions.

To further contextualize the results and enhance industrial relevance, e-methanol is compared with other major Power-to-X (P2X) products, including hydrogen, ammonia, and synthetic fuels, in terms of cost, key drivers, and end-use sectors as shown in Table 12.

Hydrogen requires dedicated infrastructure, while downstream products such as ammonia and e-methanol offer advantages in storage and transport. Among these, e-methanol occupies an intermediate cost position and benefits from compatibility with existing fuel infrastructure, making it particularly attractive for maritime transport and chemical applications. In contrast, synthetic hydrocarbons such as e-diesel and sustainable aviation fuels exhibit higher costs due to additional conversion steps and efficiency losses. Across all P2X pathways, hydrogen and electricity prices remain the dominant cost drivers, explaining much of the variability observed in the literature.

Table 12
Comparative overview of major P2X products.

P2X Product	Typical Cost Range	Key Cost Drivers	Suitable End-Use Sectors
Hydrogen (H_2) [45,46]	3000–6000 €/t	Electricity price, electrolyser CAPEX, capacity factor	Industry, refining, heavy-duty transport
Ammonia (NH_3)	600–1200 €/t	Hydrogen cost, synthesis efficiency, storage	Shipping, fertilizers, energy storage
E-meOH [42,45]	800–1400 €/t	Hydrogen cost, CO_2 supply, electricity	Shipping, chemicals, fuels
E-fuels (e-diesel/ SAF) [47]	1500–3000 €/t	Hydrogen cost, CO_2, conversion losses	Aviation, heavy transport
Conventional methanol [45, 47]	250–500 €/t	Natural gas price	Chemicals, fuels

3.3. Sensitivity to the hydrogen price

In addition to the scenario-specific comparisons discussed above, this section isolates the effect of hydrogen price on the levelized costs. Table 13 shows how variations in hydrogen price affect the LCOeM and CO_2 costs across different transport routes and modes.

As the hydrogen price increases from 2 €/kg to 8 €/kg, the LCOeM rises significantly across all scenarios, indicating that hydrogen cost is the dominant driver of overall production cost. Scenarios 1 and 3 consistently exhibit lower LCOeM values compared to scenario 2 , suggesting better cost efficiency across the tested conditions. The difference between tanker and truck transport is relatively moderate but consistent, with tanker options generally yielding slightly lower costs in most cases. In contrast, the $LCOCO_2$ remains unchanged across all scenarios, as CO_2-related costs are independent of hydrogen price variations in this analysis. Overall, the results confirm a strong sensitivity of e-MeOH economics to hydrogen pricing, while transport mode and scenario selection play a secondary but still relevant role.

4. Limitation and future scope

While comprehensive in scope, the present study has several limitations that provide directions for future research. Each scenario considers a single CO_2 emitter; incorporating multi-emitter aggregation could better balance supply variability, improve infrastructure utilization, and further reduce levelized costs through enhanced economies of scale. The transport assessment was restricted to road and maritime modes, excluding rail and pipeline alternatives that may become competitive over specific distances or flow rates. In addition, fleet size and intermediate storage capacities were not explicitly optimized, which may lead to mismatches between emission profiles and transport cycles; future work should therefore integrate dynamic fleet scheduling and storage sizing to improve cost accuracy. Capture and liquefaction costs were assumed to scale with capacity, whereas incorporating realistic scaling laws would better reflect economies of scale at larger throughputs.

Furthermore, the e-MeOH synthesis facility was fixed at a single location, limiting the ability to evaluate spatial optimization of the overall value chain. Future studies could assess alternative plant siting strategies or distributed production hubs to minimize upstream CO_2 logistics while also accounting for downstream fuel distribution. Finally, integrating low-carbon or renewable transport fuels for logistics operations would strengthen alignment with decarbonization objectives.

Table 13
Sensitivity analysis.

Hydrogen price		Scenario 1		Scenario 2		Scenario 3		Scenario 4	
		Tanker	Truck	Tanker	Truck	Tanker	Truck	Tanker	Truck
2 €/kg	LCOeM (€/t of eMeOH)	686.8	709.0	853.7	825.7	682.1	769.4	677.8	801.3
	LCO CO_2 (€/t of CO_2)	101.8	116.3	181.9	163.6	104.5	161.7	106.5	187.4
6 €/kg	LCOeM (€/t of eMeOH)	1535.7	1557.9	1702.7	1674.7	1531	1618.4	1526.8	1650.3
	LCO CO_2 (€/t of CO_2)	101.8	116.3	181.9	163.6	104.5	161.7	106.5	187.4
8 €/kg	LCOeM (€/t of eMeOH)	1960.2	1982.4	2127.2	2099.2	1955.5	2042.9	1951.3	2074.8
	LCO CO_2 (€/t of CO_2)	101.8	116.3	181.9	163.6	104.5	161.7	106.5	187.4

Despite these limitations, the study provides a systematic techno-economic framework that highlights the critical role of CO_2 availability, scale, and transport configuration in determining CCU-based e-MeOH competitiveness, thereby establishing a robust foundation for subsequent optimization and system-integration analyses.

Another limitation is the treatment of carbon pricing mechanisms. Although EUA carbon price ranges are included in the economic assumptions, avoided emissions costs associated with captured CO_2 were not credited in the LCOeM calculation. Under higher carbon price scenarios, such avoided costs could partially offset capture-related expenditures and reduce the effective net LCOeM. In addition, policy frameworks such as RED III and FuelEU Maritime are expected to strengthen demand for renewable fuels, which may further improve the economic outlook of e-MeOH systems.

5. Conclusions

Despite growing interest in CCU-based e-fuels, previous studies often rely on simplified assumptions such as constant CO_2 availability, generic feedstock inputs, and limited consideration of transport logistics, storage dynamics, and operational interdependencies. These limitations restrict the reliability of techno-economic assessments for real-world deployment. The aim of this work is to develop a comprehensive tool to quantify the overall levelized cost of e-MeOH synthesis from industrial CO_2 emitters through a full CCU value chain. The objective is twofold: to calculate the LCOCO_2 delivered to the plant and the LCOeM across realistic industrial scenarios; to identify the key parameters that determine the economic feasibility of linking hard-to-abate CO_2-emitting sectors with an e-MeOH synthesis facility. To achieve the objective, this methodology integrates a detailed process of CO_2 capture, liquefaction, transport, storage, and e-MeOH synthesis, combined with scenario-based logistics modelling to evaluate techno-economic feasibility, infrastructure requirements, and overall system performance. The study considered the cement, pulp and paper industries of Spain and Portugal as the real industrial emitters. Unlike prior studies, this framework explicitly incorporates CO_2 availability constraints, multimodal transport configurations, downtime-driven storage requirements (including loading and unloading operations), together with e-MeOH production, enabling a system-level evaluation of infrastructure utilization and cost interactions across the value chain.

The results indicate that e-MeOH synthesis dominates the overall project economics, contributing more than 80% of the total LCOeM, while CO_2 capture accounts for roughly 8–10%, and the remaining conditioning and logistics stages represent comparatively minor shares. Across all scenarios, LCOeM ranges between approximately 1100 and 1280 €/t, with the lowest value (approximately 1102.3 €/t) achieved in high-throughput cement scenarios using tanker transport. These results show that variations in LCOeM are primarily driven by CO_2 availability and transport intensity rather than processing costs. High and stable CO_2 supply (greater than 1000 kt) enables better utilization of fixed infrastructure and reduces levelized costs, whereas low-volume cases, such as approximately 150 kt, lead to underutilization and higher costs. Transport emerges as the most critical variable cost component, with tanker systems reducing logistics costs by up to 50–60% compared to road transport in long-distance scenarios. These findings highlight that previous studies underestimate the combined impact of CO_2 availability and logistics configuration on system economics. Overall, the analysis demonstrates that CO_2 source capacity, scale effects, and logistics design are the primary determinants of economic competitiveness. Therefore, feedstock availability and transport architecture must be treated as central design parameters in techno-economic assessments of CCU-based e-MeOH systems, providing a more robust basis for future research and policy development.

Overall, the results indicate that e-MeOH becomes increasingly competitive relative to fossil-derived alternatives under conditions of high carbon prices, strong low-carbon fuel mandates, and reduced hydrogen and electricity costs.

CRediT authorship contribution statement

Javier Vendrell Granero: Writing – original draft, Visualization, Software, Methodology, Investigation, Formal analysis, Data curation. **Ahmed M. Elberry:** Writing – review & editing, Validation, Supervision, Methodology, Investigation, Conceptualization. **Sayan Das:** Writing – original draft, Visualization, Methodology, Investigation. **Jagruti Thakur:** Writing – review & editing, Validation, Supervision, Resources, Methodology, Investigation, Conceptualization.

Declaration of Competing Interest

The authors declare that they have no known competing financial interests or personal relationships that could have appeared to influence the work reported in this paper.

Data availability

Data will be made available on request.

References

[1] K. Sukdolová, M. Järvinen, S. Li, F.I. Abid, J. Nyári, O. Horký, et al., Detailed techno-economic analysis of methanol synthesis from plasma assisted waste gasification derived syngas with captured CO2 at pilot scale, Energy Convers. Manag. 342 (2025) 120122, https://doi.org/10.1016/j.enconman.2025.120122.
[2] G. Tariq, Z. Chen, M. Zhao, Techno-economic and life cycle assessment of integrated bio- and e-methanol production from biomass with carbon capture and utilization, Chem. Eng. J. 515 (2025) 163850, https://doi.org/10.1016/j.cej.2025.163850.
[3] M. Crippa, D. Guizzardi, F. Pagani, M. Banja, M. Muntean, E. Schaaf, et al., GHG emissions of all world countries, Publ. Eur. Union. Luxemb. 10 (2023) 953322.
[4] A. Abdelshafy, T. Strunge, D. Stephan, G. Walther, A comparative techno-economic assessment of CO2 mineralization technologies: a case study from the construction sector, J. CO2 Util. 96 (2025) 103092, https://doi.org/10.1016/j.jcou.2025.103092.
[5] Y. Wang, Z. Wen, M. Xu, V. Kosajan, The carbon-energy-water nexus of the carbon capture, utilization, and storage technology deployment schemes: a case study in China's cement industry, Appl. Energy 362 (2024) 122991.
[6] J. Zha, Z. Li, Y. Zhang, Z. Zha, Y. Fang, P. Ma, A comparative techno-economic study of captured CO2 utilization in the cement industry in China: exploring a feasible pathway, Sustain. Energy Technol. Assess. 84 (2025) 104691, https://doi.org/10.1016/j.seta.2025.104691.
[7] A. Dubey, A. Arora, Advancements in carbon capture technologies: a review, J. Clean. Prod. 373 (2022) 133932.

[8] Y. Chang, S. Gao, Q. Ma, Y. Wei, G. Li, Techno-economic analysis of carbon capture and utilization technologies and implications for China, Renew. Sustain. Energy Rev. 199 (2024) 114550.
[9] J. Farfan, M. Fasihi, C. Breyer, Trends in the global cement industry and opportunities for long-term sustainable CCU potential for Power-to-X, J. Clean. Prod. 217 (2019) 821–835.
[10] G. Maselli, G. Oliva, A. Nesticò, V. Belgiorno, V. Naddeo, T. Zarra, Carbon capture and utilisation (CCU) solutions: assessing environmental, economic, and social impacts using a new integrated methodology, Sci. Total. Environ. 948 (2024) 174873.
[11] D. Gielen, R. Gorini, R. Leme, G. Prakash, N. Wagner, L. Janeiro, et al., World energy transitions outlook: 1.5° C pathway (2021).
[12] Y. Khojasteh-Salkuyeh, O. Ashrafi, E. Mostafavi, P. Navarri, CO2 utilization for methanol production; Part I: process design and life cycle GHG assessment of different pathways, J. CO2 Util. 50 (2021) 101608.
[13] C.A. Del Pozo, S. Cloete, Á.J. Álvaro, Techno-economic assessment of long-term methanol production from natural gas and renewables, Energy Convers. Manag. 266 (2022) 115785.
[14] European Parliament and Council of the European Union. Commission Delegated Regulation (EU) 2023/1185 of 10 February 2023 supplementing Directive (EU) 2018/2001 of the European Parliament and of the Council by establishing a minimum threshold for greenhouse gas emissions savings of recycled carbon fuels and b. Off J Eur Union 2023;157:20–32.
[15] Calvin K., Dasgupta D., Krinner G., Mukherji A., Thorne P.W., Trisos C., et al. IPCC, 2023: Climate Change 2023: Synthesis Report. Contribution of Working Groups I, II and III to the Sixth Assessment Report of the Intergovernmental Panel on Climate Change [Core Writing Team, H. Lee and J. Romero (eds.)]. IPCC, Geneva, Switzerland. 2023:35–115. ⟨https://doi.org/10.59327/IPCC/AR6-9789291691647⟩.
[16] L.F. Bobadilla, L. Azancot, M. González-Castaño, E. Ruíz-López, L. Pastor-Pérez, F. J. Durán-Olivencia, et al., Biomass gasification, catalytic technologies and energy integration for production of circular methanol: New horizons for industry decarbonisation, J. Environ. Sci. 140 (2024) 306–318.
[17] F. Yang, J.C. Meerman, A.P.C. Faaij, Carbon capture and biomass in industry: a techno-economic analysis and comparison of negative emission options, Renew. Sustain. Energy Rev. 144 (2021) 111028, https://doi.org/10.1016/j.rser.2021.111028.
[18] D.M. Fraga, R. Skagestad, N.H. Eldrup, A. Korre, H.A. Haugen, Z. Nie, et al., Design of a multi-user CO2 intermediate storage facility in the Grenland region of Norway, Int. J. Greenh. Gas. Control. 112 (2021) 103514, https://doi.org/10.1016/j.ijggc.2021.103514.
[19] S. Sollai, A. Porcu, V. Tola, F. Ferrara, A. Pettinau, Renewable methanol production from green hydrogen and captured CO2: a techno-economic assessment, J. CO2 Util. 68 (2023) 102345, https://doi.org/10.1016/j.jcou.2022.102345.
[20] A.H. Emanuelsson, J. Rootzén, F. Johnsson, Deployment of carbon capture and storage in the cement industry – Is the European Union up to shape? Int. J. Greenh. Gas. Control. 146 (2025) 104442 https://doi.org/10.1016/j.ijggc.2025.104442.
[21] H. Noh, K. Kang, International Journal of Greenhouse Gas Control Techno-economic analysis of large-scale CO 2 ship transport with onboard boil-off gas reliquefaction, Int. J. Greenh. Gas. Control. 142 (2025) 104337, https://doi.org/10.1016/j.ijggc.2025.104337.
[22] Lorin, et al., A mature business opportunity to enhance sustainable carbon cycles and untap the circularity and climate benefits of biogas production, Eur. Biogas Assoc. 2019 (2019).
[23] K. Kuparinen, E. Vakkilainen, T. Tynjälä, Biomass-based carbon capture and utilization in kraft pulp mills, Mitig. Adapt. Strateg. Glob. Chang. 24 (2019) 1213–1230, https://doi.org/10.1007/s11027-018-9833-9.
[24] K. Onarheim, S. Santos, P. Kangas, V. Hankalin, Performance and costs of CCS in the pulp and paper industry part 1: Performance of amine-based post-combustion CO2 capture, Int. J. Greenh. Gas. Control. 59 (2017) 58–73, https://doi.org/10.1016/j.ijggc.2017.02.008.
[25] SCHWENK Zement, SkyNRG, Stuttgart Airport. Assessment of European biogenic CO 2 balance for SAF production 2022.
[26] BIP Europe T 4. Biogenic CO2: The role of the biomethane industry in satisfying a growing demand 2024.
[27] S.M.N. Hassan, Techno-Economic Study of CO2 Capture Process for Cement Plants (2005) 1–200.
[28] A.N. Antzaras, T. Papalas, E. Heracleous, C. Kouris, Techno–economic and environmental assessment of CO2 capture technologies in the cement industry, J. Clean. Prod. 428 (2023) 139330, https://doi.org/10.1016/j.jclepro.2023.139330.
[29] C.-C. Cormos, Decarbonization options for cement production process: a techno-economic and environmental evaluation, Fuel 320 (2022) 123907, https://doi.org/10.1016/j.fuel.2022.123907.
[30] A. Parkhi, S. Cremaschi, Z. Jiang, Techno-economic analysis of CO2 capture from Pulp and paper Mill Limekiln, IFAC-PapersOnLine 55 (2022) 284–291, https://doi.org/10.1016/j.ifacol.2022.07.458.
[31] H. Gerbelová, M. van der Spek, W. Schakel, Feasibility assessment of CO2 capture retrofitted to an existing cement plant: post-combustion vs. oxy-fuel combustion technology, Energy Procedia 114 (2017) 6141–6149, https://doi.org/10.1016/j.egypro.2017.03.1751.
[32] C. Schoeneberger, J. Zhang, C. McMillan, J.B. Dunn, E. Masanet, Electrification potential of U.S. industrial boilers and assessment of the GHG emissions impact, Adv. Appl. Energy 5 (2022) 100089, https://doi.org/10.1016/j.adapen.2022.100089.
[33] A. Haar, Van De, C. Trapp, K. Wellner, R.De Kler, G. Schmitz, P. Colonna, Dynamics of Postcombustion CO 2 Capture Plants, Model. Valid. Case Study (2017), https://doi.org/10.1021/acs.iecr.6b00034.
[34] Ziobrowski Z., Rotkegel A. Comparison of CO 2 Separation Efficiency from Flue Gases Based on Commonly Used Methods and Materials 2022.
[35] D. Gosse, Press release Industrial Heat Bosch Industrial Heat at ISH The new Bosch ELHB electric boiler for heating (2025).
[36] European Comission. Carbon capture, storage and utilisation 2024.
[37] Short, W., Packey, D. J., & Holt, T. (1995). A Manual for the Economic Evaluation of Energy Efficiency and Renewable Energy Technologies. National Renewable Energy Laboratory (NREL), NREL/TP-462-5173. Golden, CO, USA.
[38] HM Treasury (2024) Green Book supplementary guidance: discounting. London: HM Treasury. Available at: https://www.gov.uk/government/publications/green-book-supplementary-guidance-discounting.
[39] S. Dietz, W. Irwin, B. Rauis, V. Jahn, J. Noels, V. Komar, R. Goon, Carbon Performance assessment of paper producers: methodology note, LSE Research Online Documents on Economics, LSE Research Online Documents on Economics (2021).
[40] IEA, 2023. Tracking Cement. URL https://www.iea.org/energy-system/industry/cement (accessed 6.14.24).
[41] Omar, Ara and Widgren J. Cost-Optimization and Feasibility of e-Methanol Production Powered by Offshore Wind Energy 2025.
[42] Hank C., Holst M., Thelen C., Kost C., Längle S. Site-specifi c, comparative analysis for suitable Power-to-X pathways and products in developing and emerging countries n.d.
[43] G. Liu, B. Cai, Q. Li, X. Zhang, China's pathway of CO2 cpature, utilization and storage under carbon neutrality vision 2060, Carbon Management. 13 (1) 435–449. https://doi.org/10.1080/17583004.2022.2117648.
[44] Xing Y., Aditya T., Santoso D., Ma Y. Technical – Economic Feasibility Analysis of Subsea Shuttle Tanker 2022.
[45] B. Engineering, BSc in Chemical and Biochemical Engineering Comparative cost analysis of different CO 2 Capturing, Storage and Transport modes in 2023 (2023).
[46] G. Cook, Next Generation Carbon Capture Technology Verified by 2022 (2022).
[47] Liana Gouta, Statistical Report of Europe Fuel Scenario (2025).
[48] Evaluation of Retrofitting CCS in a Market Pulp Integrated Pulp Report: 2016 / 10 2016.
[49] J. Gervasi, L. Dubois, D. Thomas, Simulation of the post-combustion CO2 capture with aspen HysysTM software: study of different configurations of an absorption-regeneration process for the application to cement flue gases, Energy Procedia 63 (2014) 1018–1028, https://doi.org/10.1016/j.egypro.2014.11.109.
[50] P. Dogliani, A.N. Ruas Rego Canha, A.M. Elberry, J. Thakur, Multi-option analytical modeling of levelized costs across various hydrogen supply chain nodes, Int. J. Hydrog. Energy 70 (2024) 737–755, https://doi.org/10.1016/j.ijhydene.2024.05.142.
[51] Y. Gu, D. Wang, Q. Chen, Z. Tang, Techno-economic analysis of green methanol plant with optimal design of renewable hydrogen production: a case study in China, Int. J. Hydrog. Energy 47 (2022) 5085–5100, https://doi.org/10.1016/j.ijhydene.2021.11.148.
[52] M. Pérez-Fortes, J.C. Schöneberger, A. Boulamanti, E. Tzimas, Methanol synthesis using captured CO2 as raw material: techno-economic and environmental assessment, Appl. Energy 161 (2016) 718–732, https://doi.org/10.1016/j.apenergy.2015.07.067.
[53] R. Svensson, M. Odenberger, F. Johnsson, L. Strömberg, Transportation systems for CO2—application to carbon capture and storage, Energy Convers. Manag. 45 (2004) 2343–2353, https://doi.org/10.1016/j.enconman.2003.11.022.
[54] C.-C. Cormos, Oxy-combustion of coal, lignite and biomass: a techno-economic analysis for a large scale Carbon Capture and Storage (CCS) project in Romania, Fuel 169 (2016) 50–57, https://doi.org/10.1016/j.fuel.2015.12.005.
[55] M.S. Peters, K.D. Timmerhaus, R.E. West, Plant design and economics for chemical engineers (2003).
[56] EBA. Biogenic CO2 from biogases: key to Europe's carbon strategy 2025:1.
[57] International Renewable Energy Agency, "Innovation Outlook Renewable", 2024, Accessed on 04/05/2026.
[58] D. Lin, L. Zhang, C. Pan, H. Hu, J. Yang, B. Tong, et al., Techno-economic analysis of offshore green methanol production in South China Sea, Chem. Eng. J. 527 (2026) 171867, https://doi.org/10.1016/j.cej.2025.171867.